PHYS 4620 Final Year Project Report
Rabi Oscillation and State Construction in Quantum Bouncing Ball System

Shing Chau (John) Leung,
Supervised by Prof. C.K. Law

Department of Physics,
the Chinese University of Hong Kong,
Hong Kong

May 7, 2012

Abstract

The quantum bouncing ball system is one of the recent experiments addressing the quantum behavior of a particle interacting with gravity. Such a system is constructed through passing ultra-cold neutrons into an oscillation platform, on which the neutron interacts with the earth's gravitational potential, mgz, and an oscillating reflective ground surface.

In this project, we investigate how the oscillating surface induces Rabi oscillations between different excited states of the system. In addition, we present a method to generate general quantum superposition states by manipulating the oscillations of the ground boundary.

1 Introduction

The quantum bouncing ball system is a quantum mechanical analogy of a classical bouncing ball. The system consists of a particle in the Earth's gravitational potential (mgz), and a reflective ground surface. In the Schrödinger equation, we can easily decouple the axis parallel to gravity, the z-axis, of the system from the xy-axis (see Section 3.1). The Hamiltonian of the quantum bouncing ball is as follow:

$$H = \frac{p^2}{2m} + mgz + V_0\Theta(-z) \tag{1}$$

g is the surface strength of the Earth's gravitation field. V_0 is a potential barrier many orders of magnitude large then the mgz potential. It reflects the particle away from the surface, giving it a 'bouncing' effect. [3]

The eigenstates of the Hamiltonian (1) can be described by Airy functions. The first 3 eigenstates are plotted in Fig. 1 The eigenenergies are of several peVs. The solution of this system will be studied in detail in Part 2 of this report.

In general, the position of the reflecting surface along z-axis can depend on the time. We can introduce a time-dependent function $f(t)$ in the position of the ground potential barrier V_0. This means that the ground potential barrier is oscillating and can induce states transition in the quantum system. Now the time-dependent Hamiltonian can be written as:

$$H(t) = \frac{p^2}{2m} + mgz + V_0\Theta(f(t) - z) \tag{2}$$

In this project, we are interested in studying the state transition driven by a sinusoidal boundary, i.e. $f(t) = \sin(\omega t)$. We have learnt that we under small oscillation amplitude, we can approximation these transitions as a set of Rabi oscillations between different excited states of the system. Thus, we will manipulate the oscillations of the ground boundary, in an attempt to construct interesting superpositions of several eigenstates.

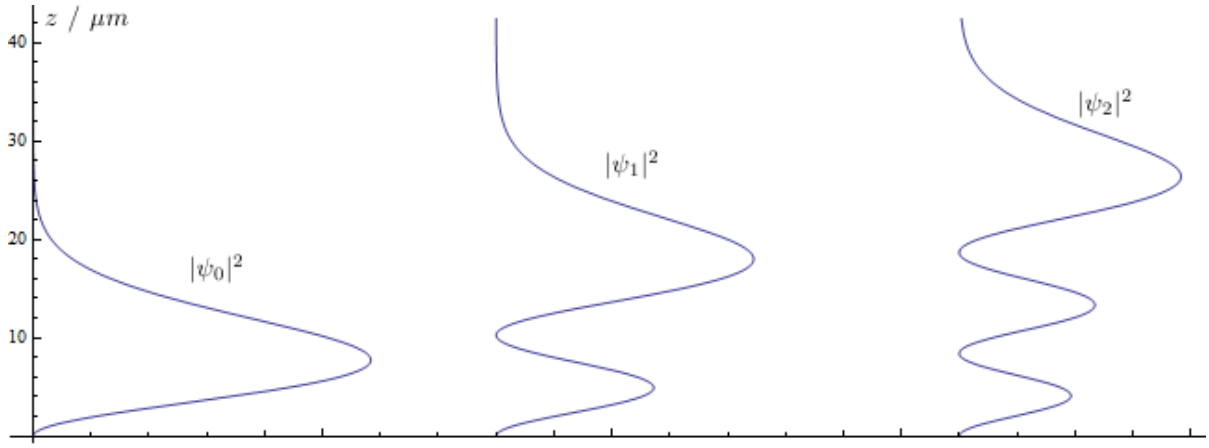

Figure 1: From left to right, the probability function of the ground state, first excited and second excited state of the Hamiltonian H.

2 Experiment Setup

The quantum bouncing ball had been difficult to realize in the past owning to the weakness of the Earth's gravitational field. Since the energies of gravitational bound states are of pico-electronvolts scale, any stray electromagnetic interaction would destroy the gravitational quantum effect we wish to investigate completely.

Until recent years, quantum bouncing ball system has been successfully constructed by using neutrons [5], [1]. The experiment setup is *qBounce*, constructed by Hartmut Abele and his group within Atominstitut of Technische Universität Wien in Vienna, Austria. The setup prevents the quantum system from influence of any electromagnetic interactions and thermal noises by using chargeless, ultra-cold neutrons. Through that, this setup realized the quantum bouncing ball system described by Hamiltonian in Eq. (2).

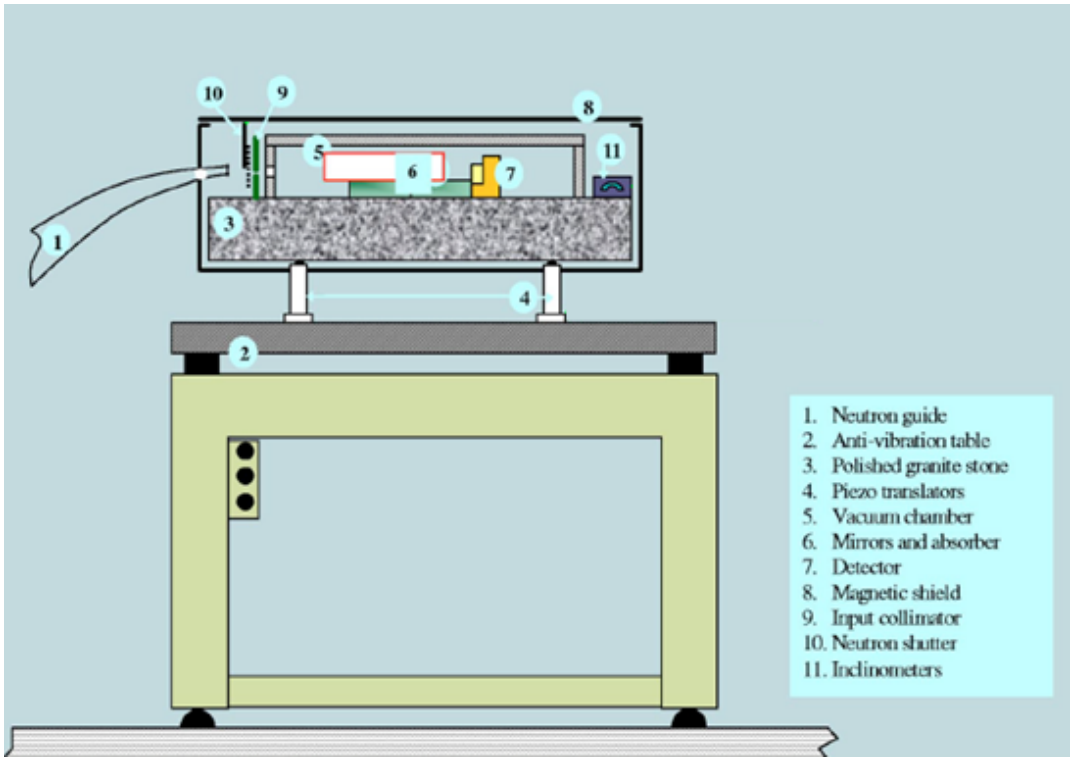

Figure 2: A schematic diagram of qBounce [5]

The setup admits cold electron of velocities ranging from 3 m/s to 20 m/s. Thus, it provides neutron trapping time of ∼10 ms. The neutron shutter within the setup select neutrons with low energy and low vertical momentum. Also, the whole setup is protected by a magnetic shield to prevent external magnetic field coupling to neutron's spin.

The setup has a 15 cm quantum evolution area in which cold neutrons' time evolution can be described by the Hamiltonian in Eq. (2). The evolution area is a small slit located within the vacuum chamber, sandwiched between the neutron absorber (the white rectangle with red rim in Fig. 2) and the neutron mirror (the green rectangle just below the absorber). A schematic diagram for the evolution area is in Fig. 3 below.

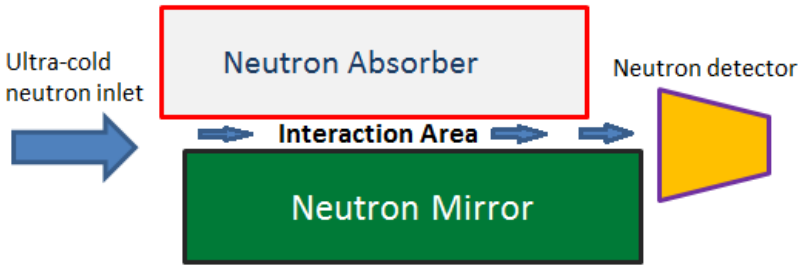

Figure 3: A schematic diagram of the evolution area of qBounce

Fig. 3 is the enlarged version of the component 6 in Fig. 2. The neutron mirror is made of polished granite. At all incident angles, the mirror reflects neutrons with very long wavelength perfectly. It acts as the ground potential barrier in Eq. 1. The neutron absorber is made of Ti-Zr-Gd alloy which height can be adjusted. This means the the width of the middle interaction area can be varied. According to Fig. 1, the height of the wavefunction increases as the neutron climbs into more excited states. The variable width of the interaction area means that one can select the number of states admitted into the system, counting from the ground state. For example, if the separation of the absorber and the mirror is as small as 18 μm, only ground state will survive inside the system.

The qBounce experiment has verified that the time evolution of quantum bouncing ball indeed follows the Hamiltonian in Eq. (1). With the success of qBounce setup, an upgraded quantum bouncing ball system, with extended evolution area length and an oscillating ground mirror, is proposed. A diagram of the proposed upgraded setup is drawn below:

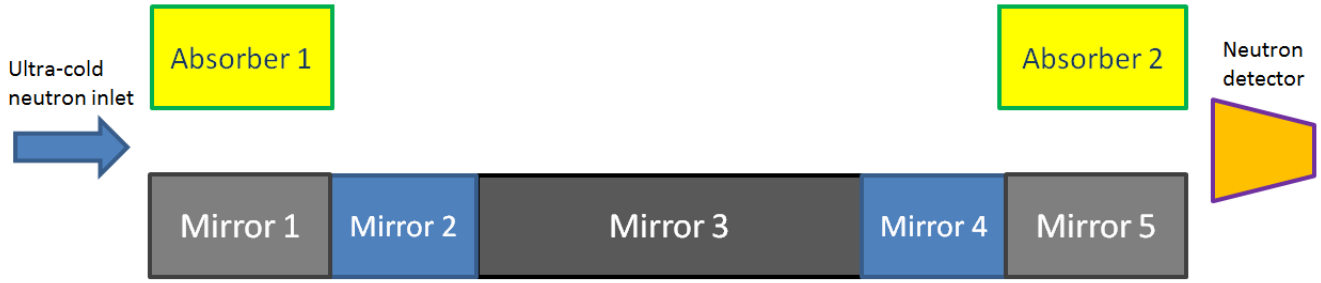

Figure 4: Proposed upgraded setup for gravitational spectroscopy [4], [2]

The new setup has a several additional neutron mirrors. They can be programmed to vibrate at some specific frequencies. This type of mirror correspond to an oscillating ground boundary described in the Hamiltonian in Eq. (2). We will show that such oscillating ground can induce state transition. In particular, if the driving oscillation frequency is the resonance frequency between two of the energy levels, the system will behave like a two-level system and will perform Rabi oscillation between the two corresponding resonance states. We make use of such properties to construct particular superposition of states.

3 Solving Schrödinger Equation for Quantum Bouncing Ball

3.1 Deriving 1D Quantum Bouncing Ball's Schrödinger Equation

We want to solve the time dependent Schrödinger equation of the quantum bouncing ball system.

$$H|\psi\rangle = i\hbar\frac{\partial}{\partial t}|\psi\rangle \tag{3}$$

where H is the Hamiltonian in Eq. 2. We can expand H in Cartesian Coordinates.

$$H = -\frac{\hbar^2}{2m}\left(\frac{\partial^2}{\partial x^2} + \frac{\partial^2}{\partial y^2} + \frac{\partial^2}{\partial z^2}\right) + V(z,t) \tag{4}$$

and

$$V(z,t) = mgz + V_0\Theta(f(t) - z) \tag{5}$$

Obviously, the x, y dependence of the Hamiltonian is just that of a free particle. Using separation of variables, the motion along x and y direction is plane wave. Let

$$\psi(\vec{r},t) = X(x)Y(y)Z(z,t) \tag{6}$$

solutions for X and Y are

$$X(x) = \exp(ik_x x) \tag{7a}$$

$$Y(y) = \exp(ik_y y) \tag{7b}$$

Now we can consider the equation for z-axis independently,

$$\left\{-\frac{\hbar^2}{2m}\left(\frac{\partial^2}{\partial z^2} - k_x^2 - k_y^2\right) + V(z,t)\right\} Z(z,t) = i\hbar\frac{\partial Z(z,t)}{\partial t} \tag{8}$$

Equation (8) itself constitutes a Schrödinger equation. We can consider $Z(z,t)$ itself as a wavefunction $\psi(z,t)$ with some extra constant energies contributed by its horizontal momentum. Since the k_x and k_y are not coupled with $Z(z,t)$ equation, we can ignore the k_x^2 and k_y^2 terms by resetting the ground energy. And hence we get an 1-D quantum bouncing ball Hamiltonian:

$$\left(-\frac{\hbar^2}{2m}\frac{\partial^2}{\partial z^2} + V(z,t)\right)\psi(z,t) = i\hbar\frac{\partial\psi(z,t))}{\partial t} \tag{9}$$

3.2 Solutions for Time-Independent Schrödinger Equation

First of All, we want solve the stationary state of Hamiltonian (1), in which we write

$$p = -i\hbar\frac{\partial}{\partial z} \tag{10}$$

from the argument in Section 3.1. Hamiltonian (1) can be written a Hamiltonian without the ground potential V_0, but we impose a boundary condition on the Schr"odinger equation such that $\psi(z) = 0$ at $z \leq 0$. In addition, we need $\psi(z) = 0$ at $z \to \infty$ for bounded states.

We rewrite the Schrödinger equation in a dimensionless form. By introducing the characteristic length

$$\ell = \left(\frac{\hbar^2}{2m^2 g}\right)^{\frac{1}{3}} \tag{11}$$

We put the mass of the particle as the mass of a neutron ($m = 1.675 \times 10^{-27} kg$) and g as standard gravity ($9.807\ m/s^{-2}$). We can carry out the following rescaling:

$$z \longmapsto \frac{z}{\ell} \tag{12a}$$

$$t \longmapsto \frac{mg\ell}{\hbar} \tag{12b}$$

$$E \longmapsto \frac{E}{mg\ell} \tag{12c}$$

One unit of such 'characteristic' length is 5.86 μm, of time is 1.10 ms, and of energy is 0.60 peV.

The dimensionless eigenvalue equation we wish to solve is now formulated as

$$-\frac{\partial^2\psi}{\partial z^2} + z\psi = E\psi \qquad\qquad \psi = 0 \text{ at } z \leq 0 \tag{13}$$

Above $z = 0$, the eigenstates of Eq. (13) can be described by Airy function of the first kind (Ai), defined by

$$Ai(z + \zeta_n) = \frac{1}{\pi}\int_0^\infty \cos\left(\frac{1}{3}s^3 + (z + \zeta_n)s\right) ds \tag{14}$$

with ζ_n being the nth zero of the Airy function.

$$Ai(\zeta_n) = 0 \qquad\qquad \text{for integer } n > 0 \tag{15}$$

The first 3 eigenstate probability functions are plotted in Fig. 1 on the first page.

Each eigenstate function $Ai(z+\zeta_n)$ corresponds to an eigenenergy E_n. The first 5 eigenenergies of the solution are $\{1.41, 2.46, 4.08, 4.78\}$ in peV. First 30 energy states are plotted in Fig. 5. The eigenenergy curve has a dependence of $E_n \propto \left(n - \frac{1}{4}\right)^{2/3}$. [5]

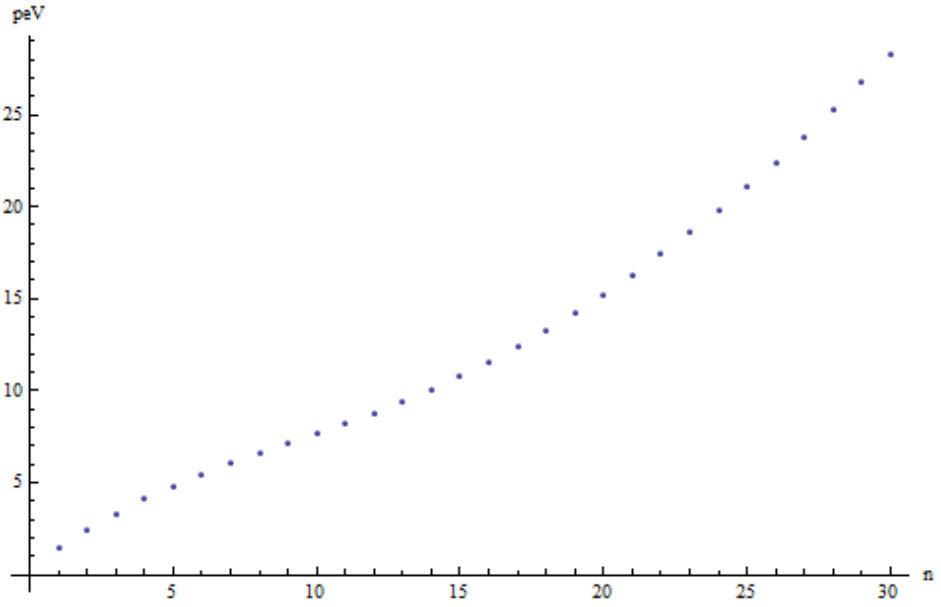

Figure 5: First 30 eigenenergies of the quantum bouncing ball system

Off by a trivial normalization factor, $Ai(z + \zeta_n)$ are the complete set of eigenstates of this system. Airy function of the second kind (Bi) is not admissible since it diverges as $z \to \infty$.

3.3 Solutions for Time-Dependent Schrödinger Equation

To discuss about state transition, we introduce an oscillation ground for the quantum bouncing ball system as in Eq. (2). The oscillation function $f(t)$ has an oscillation amplitude a and frequency ω. Using the same set of dimensionless units in (12).

We can write the time-dependent Schrödinger equation as

$$-\frac{\partial^2\psi}{\partial z^2} + [z + V_0\Theta(a\sin(\omega t) - z)]\psi = i\frac{\partial\psi}{\partial t} \tag{16}$$

Similar to the time-independent case, since $V_0 \gg 1$, we instead consider the Schrödinger equation

$$-\frac{\partial^2\psi}{\partial z^2} + z\psi = i\frac{\partial\psi}{\partial t} \tag{17}$$

with the time-dependent boundary condition

$$\psi(z,t) = 0 \qquad \text{for } z < a\sin(\omega t) \tag{18}$$

Eq. (17) is the same as Eq. (13) apart from a change in boundary condition. It is convenient use the old solutions Eq. (13) but replace z with a time-dependent variable that suits the boundary condition. i.e.

$$z \longmapsto z - a\sin(\omega t) \tag{19}$$

The set of normal modes we considered are,

$$u_n(z,t) = \frac{1}{\mathcal{N}_n} Ai(z + \zeta_n - a\sin(\omega t)) \qquad \text{for } z > a\sin(\omega t) \tag{20}$$

where $\mathcal{N}_n$ is a normalization factor for the nth normal mode. The time-dependent normal modes in (20) can be considered as observing a system with a reference frame that is co-moving with the oscillation ground. In general, a state ψ is represented by a superposition of such normal modes,

$$\psi(z,t) = \sum_{n=1}^{\infty} c_n(t) u_n(z,t) \tag{21}$$

Plugging in the state (21) into (17),

$$\sum_m (\omega_m + a\sin(\omega t)) c_m u_m = i\sum_m (\dot{c}_m u_m + c_m \dot{u}_m) \tag{22}$$

In our dimensionless units, $\omega_m = E_m$ which is the eigenvalues in Eq. (13). And ω is our driving frequency.

If we multiply Eq. (22) by u_n and integrate along z-axis, we get the following relation

$$(\omega_n + a\sin(\omega t)) c_n - ia\omega\cos(\omega t)\sum_m c_m Q_{n,m} = i\frac{dc_n}{dt} \tag{23}$$

where Q is an anti-hermitian matrix with matrix element

$$Q_{n,m} = \int_0^\infty \frac{1}{\mathcal{N}_n \mathcal{N}_m} \frac{dAi(z+\zeta_m)}{dz} Ai(z+\zeta_n) dz \tag{24}$$

The integrals are evaluated by numerical integration. Below shows the first 5×5 terms:

	$Q_{m,n}$				
	$m=1$	$m=2$	$m=3$	$m=4$	$m=5$
$n=1$	0	0.571	-0.314	0.224	-0.178
$n=2$	-0.571	0	0.700	-0.371	0.259
$n=3$	0.314	-0.700	0	0.790	-0.413
$n=4$	-0.224	0.371	-0.790	0	0.864
$n=5$	0.178	-0.259	0.413	-0.864	0

Table 1: Numerical values of matrix elements of Q

Matrix Q has zero diagonal elements and has off-diagonal elements of magnitude $|Q_{n,m}| < 1$. The value of $Q_{n,m}$ decreases as the difference between n and m increases.

Eq. (23) is an m-coupled ordinary equation. Although numerical solution can be calculated directly by truncating large m mode, the equation will be more useful for proving our Rabi oscillation approximation in the next section.

4 Rabi Oscillation in Quantum Bouncing Ball

4.1 Rotating Frame Approximation

In this section, we will show that quantum bouncing ball with an sinusoidal oscillating boundary behavior like a 2-level Rabi system given the 2 conditions that

- the driving frequency resonances with the energy difference between the two pertinent normal modes; (e.g. $\omega \approx \omega_1 - \omega_2$)
- the amplitude of the ground oscillation is small. (i.e. $a \ll 1$)

For simplicity, we first consider that a state ψ in a 2-state space. The two states are chosen to be the ground state (u_0) and the first excited state (u_1) in the following discussion, though the argument can be easily generalized to any two modes u_n and u_m.

$$|\psi\rangle = \begin{pmatrix} c_1 \\ c_0 \end{pmatrix} \tag{25}$$

the definitions of c_1 and c_0 are consistent with those in Eq. (21)

The time evolution equation is

$$(\mathbf{H}_0 + a\sin(\omega t) - ia\omega\cos(\omega t)\mathbf{Q})|\psi\rangle = i\frac{d}{dt}|\psi\rangle \tag{26}$$

In 2-state form,

$$\mathbf{H}_0 = \begin{pmatrix} \omega_1 & 0 \\ 0 & \omega_0 \end{pmatrix} \tag{27}$$

and

$$\mathbf{Q} = \begin{pmatrix} 0 & q \\ -q & 0 \end{pmatrix} \tag{28}$$

where $q = Q_{2,1} = -Q_{1,2} \approx 0.571$.

The two corespondent equations, written explicitly, are

$$(\omega_0 + a\sin(\omega t))c_0 + iaq\omega\cos(\omega t)c_1 = i\dot{c}_0 \tag{29a}$$

$$(\omega_1 + a\sin(\omega t))c_1 - iqa\omega\cos(\omega t)c_0 = i\dot{c}_1 \tag{29b}$$

Equation (29) can be simplified by the follow procedures. We define two coefficients, $\tilde{c}_0$ and $\tilde{c}_1$, in rotating frame,

$$\tilde{c}_0 = c_0 \exp\left(i\omega_0 t - i\frac{a}{\omega}\cos(\omega t)\right) \tag{30a}$$

$$\tilde{c}_1 = c_1 \exp\left(i(\omega_0+\omega) t - i\frac{a}{\omega}\cos(\omega t)\right) \tag{30b}$$

Writing $\Delta\omega_{10} = \omega_1 - \omega_0$, the above change of variables simplify the eq. (29) to

$$\frac{iaq\omega}{2}\left(e^{-i(2\omega)t} + 1\right)\tilde{c}_1 = i\dot{\tilde{c}}_0 \tag{31a}$$

$$(\Delta\omega_{10} - \omega)\tilde{c}_1 - \frac{iaq\omega}{2}\left(1 + e^{i(2\omega)t}\right)\tilde{c}_0 = i\dot{\tilde{c}}_1 \tag{31b}$$

The exponential terms, $\exp(\pm 2i\omega t)$, in Eq. (31) are rapid oscillating terms given $\omega \sim \Delta\omega_{01}$. Naturally, $2\omega \gg \omega - \Delta\omega_{10}$. We can apply rotating frame approximation. i.e., the exponential terms can be neglected.

$$\frac{iaq\omega}{2}\tilde{c}_1 = i\dot{\tilde{c}}_0 \tag{32a}$$

$$(\Delta\omega_{10} - \omega)\tilde{c}_1 - \frac{iaq\omega}{2}\tilde{c}_0 = i\dot{\tilde{c}}_1 \tag{32b}$$

We are now well-equipped to write out quantum bouncing ball in Rabi oscillation terms.

4.2 Resonance and Detuning

Let's write Eq. (32) in matrix form:

$$\begin{pmatrix} \Delta\omega_{10} - \omega & -i\Omega \\ i\Omega & 0 \end{pmatrix} |\psi\rangle = i\frac{d}{dt}|\psi\rangle \tag{33}$$

where

$$\Omega = \frac{aq\omega}{2} \tag{34}$$

which is, indeed, a Schrödinger equation of Rabi two-level system.

Suppose we tune the driving frequency ω to exact resonance with the two levels, i.e. $\omega = \Delta\omega_{10}$. Eq. (33) becomes

$$\begin{pmatrix} 0 & -i\Omega \\ i\Omega & 0 \end{pmatrix} |\psi\rangle = i\frac{d}{dt}|\psi\rangle \tag{35}$$

Given the initial condition $\tilde{c}_0 = 1$ and $\tilde{c}_1 = 0$, the solutions of Eq. (35) for $\tilde{c}_0$ and $\tilde{c}_1$ are

$$\tilde{c}_0 = \cos(\Omega t) \tag{36a}$$

$$\tilde{c}_1 = \sin(\Omega t) \tag{36b}$$

Let the oscillation amplitude $a = 0.05$, which in SI unit is 0.29 μm. The corresponding Rabi frequency Ω is 45.7 s^{-1}. The oscillation pattern of the ground state probability is plotted in Fig. 6a.

If the resonance is not exact, i.e. $\omega \neq \Delta\omega_{10}$, the Rabi oscillation will not transit the probability from ground state to the excited state completely. The time evolution of such inexact resonance is governed by

$$\begin{pmatrix} \delta & -i\Omega \\ i\Omega & 0 \end{pmatrix} |\psi\rangle = i\frac{d}{dt}|\psi\rangle \tag{37}$$

where

$$\delta = \Delta\omega_{10} - \omega \tag{38}$$

which is just the same equation as (33). But we renamed the upper left matrix element of the Hamiltonian as δ, the detuning. Detuning is a measure of how far away the driving frequency is from the resonance frequency of the two-level state. The more detuned the driving frequency is, the less transition between the two states there would be. This can be observed explicitly in Fig. 7.

We want to formally address the problem whether we can actually consider the quantum bouncing ball system as a two-level system for some Rabi frequencies. i.e. whether the assumption in Eq. (23) holds, and with which Rabi frequencies it holds.

When we are doing Rabi oscillation between the ground state and first excited state, we must see how much probability will 'leak' to higher excited states, such as second excited state. We set the driving frequency ω to the resonance frequency of the ground state and first excited state $\Delta\omega_{10}$, but instead of consider the ground state and first excited state as our 2-level system, we consider the ground state and the second excited state as our two-level system. Thus we have a detuning of the form

$$\delta = \Delta\omega_{10} - \Delta\omega_{20} \tag{39}$$

which is about 57Ω.

With large detuning in the states other than the two resonances states, probability 'leakage' can be prevented. The larger this detuning is, the better the two-level approximation of the ground state and first excited state is. From Fig. 7, $\delta > 5\Omega$ is a good criterion for a good two-level approximation. Certainly, we have to consider the leakage of probability to other excited state also, for instance, from ground state to third excited state ($\delta = \Delta\omega_{10} - \Delta\omega_{30}$), and from first excited state to second excited state ($\delta = \Delta\omega_{10} - \Delta\omega_{21}$), etc.

To systematically calculate how good our 2-level approximation is, we can tabulate the values of δ between different levels in different two-levels system.

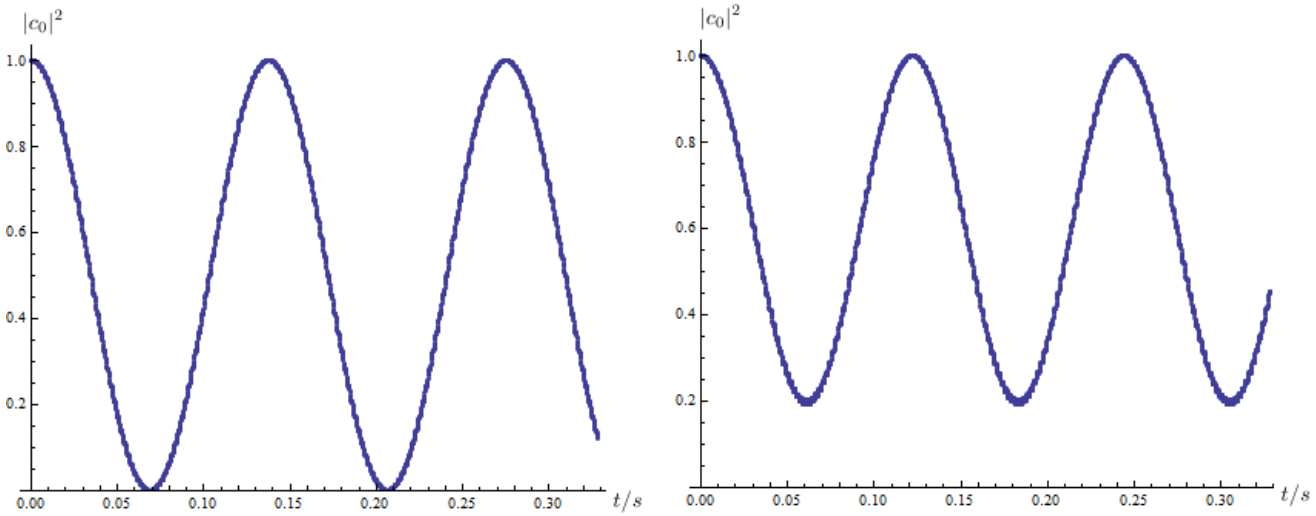

(a) Exact Resonance: $\delta = 0$

(b) Detuned: $\delta = \Omega$

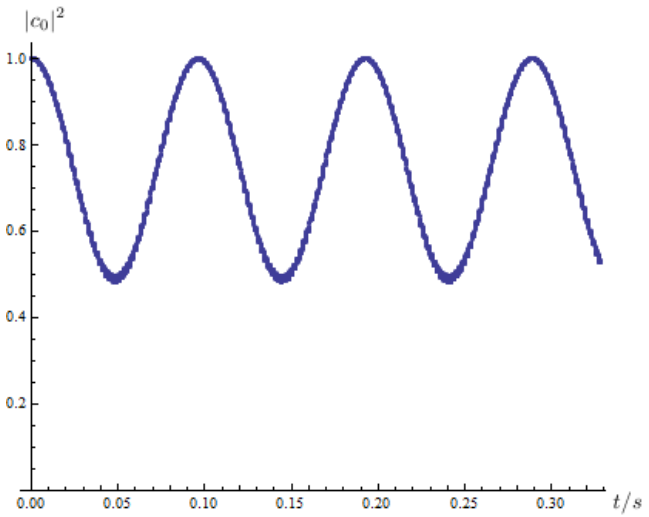

(c) Detuned: $\delta = 2\Omega$

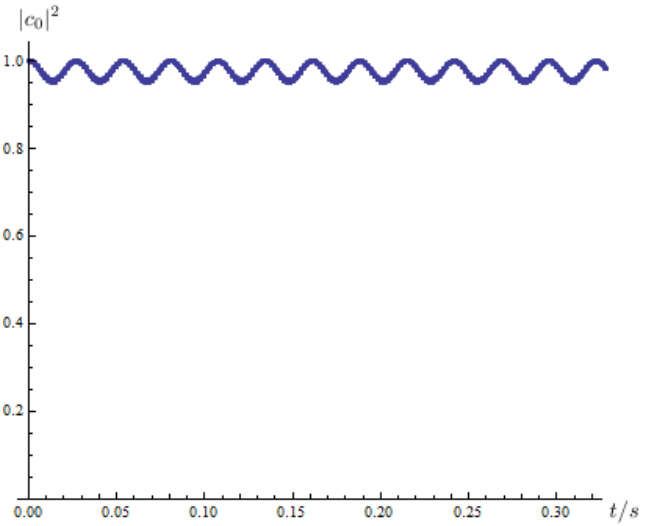

(d) Detuned: $\delta = 5\Omega$

Figure 6: Oscillation of ground state probability with different magnitudes of detuning (δ)

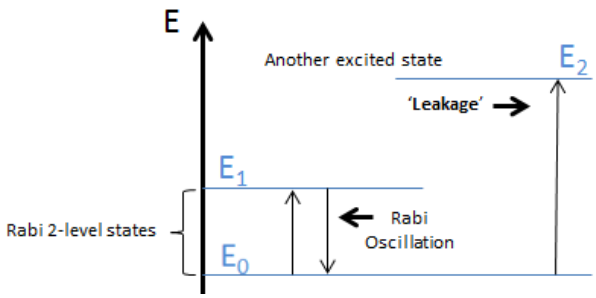

(a) Leakage (arrows represent transfer of amplitude)

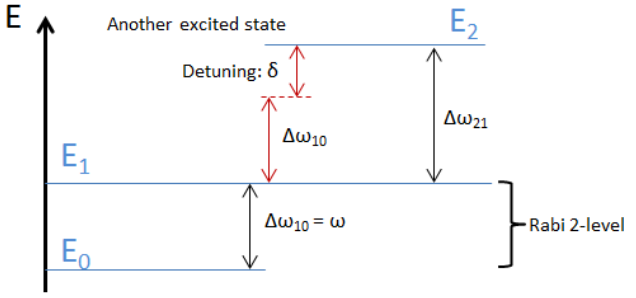

(b) Detuning δ that prevents leakage

Figure 7: Energy level diagram expression of 'leakage' and prevention of leakage through detuning

The table reads as *Column* minus *Row*. i.e. the box in the third column and fourth row represents the value $\Delta\omega_{32} - \Delta\omega_{43}$, which is the leakage to the fourth excited state from the third excited during a third-second excited state Rabi oscillation.

The leakage to second excited state from first excited state during a ground-first excited state Rabi

δ/Ω	ω_{10}	ω_{21}	ω_{32}	ω_{43}	ω_{54}
ω_{10}	0	13	19	24	26
ω_{21}	-13	0	7	11	14
ω_{32}	-19	-7	0	4	8
ω_{43}	-24	-11	-4	0	3
ω_{54}	-26	-14	-8	-3	0

Table 2: Values of δ of adjacent level leakage in Rabi oscillation of 2 adjacent levels

oscillation is characterized by the detuning $\delta = \Delta\omega_{10} - \Delta\omega_{21}$, which is the detuning in the first row, second column. It reads $\delta = 13\Omega$.

According to the table, when doing Rabi oscillation between third excited state and second excited state, it is likely that probability will leak into the fourth excited state, because the detuning δ is only 4Ω. Since it is only the value δ/Ω that matters, we can raise the detuning to a 'safe level' by decreasing the magnitude of Ω. From Eq. (34), we can do so by lowering the oscillation amplitude of the ground a.

Table 2 only accounts for detunings δ that concern a leakage of probability amplitude between adjacent levels. For example, the table would not account for leakage from the first excited state to third excited state during a ground-second excited state oscillation. Of course we can plot such table as in Table 3 and all other modes of leakage and Rabi oscillation. For the conciseness of this report, we only plot one more table which shows the values of δ of 1-level separation leakage in Rabi oscillation of 1-level separated Rabi oscillation.

δ/Ω	ω_{20}	ω_{31}	ω_{42}	ω_{53}	ω_{64}
ω_{20}	0	-19	-30	-38	-87
ω_{31}	19	0	-11	-65	-67
ω_{42}	30	11	0	-8	-13
ω_{53}	38	65	8	0	-6
ω_{64}	87	67	13	6	0

Table 3: Values of δ of 1-level separation leakage in Rabi oscillation of 1-level separated Rabi oscillation

With a good monitor of probability leakage using detuning, we are ready for constructing interesting states of superposition.

5 State Construction with Rabi Oscillation

5.1 Method and Result for Example State ψ_{123}

We wish to construct interesting quantum superposition of states in the basis of u_n in Eq. (20), through Technique we have developed in the previous section. State construction is a procedure that: 1.) a known input state is known. 2.) the state is modified with some Hamiltonian we can manipulate. 3.) a specific state we want is output.

$$\psi_{input} \longrightarrow e^{-iHt}\psi \longrightarrow \psi_{output} \tag{40}$$

As an example, we want to construct a 3-level equally populated state, which involves the first 3 levels of equal amplitude. In short, we call it 123-state (ψ_{123}).

$$\psi_{123}(t) = \frac{1}{\sqrt{3}}(u_1 + u_2 + u_3) \tag{41}$$

We chose our input initial state to be the ground state u_0.

$$\psi(t=0) = u_0 \tag{42}$$

It is know that through setting the driving frequency ω to $\Delta\omega_{10}$, we can transport the probability amplitude from ground state to first excited state u_1. Suppose we apply a pulse of oscillation that last for τ_{01}, such that u_1 only acquire an amplitude of $\frac{1}{\sqrt{3}}$. It means that we maintain the ground oscillating until Rabi oscillation gives us the state below at $t = \tau_{01}$.

$$\psi(\tau_{01}) = \left(1 - \frac{1}{\sqrt{3}}\right) u_0 + \frac{1}{\sqrt{3}} u_1 \tag{43}$$

After that, we immediately change the driving frequency from $\omega = \Delta\omega_{10}$ to $\omega = \Delta\omega_{21}$. The Rabi oscillation between u_0 and u_1 stops, and Rabi oscillation between u_0 and u_2 commences. Again, we drive the system for τ_{12}. Until the system reaches the state

$$\psi(\tau_{01} + \tau_{12}) = \frac{1}{\sqrt{3}} u_0 + \frac{1}{\sqrt{3}} u_1 + \frac{1}{\sqrt{3}} u_3 \tag{44}$$

We stop the oscillation of the ground completely. Now the wavefunction is allowed to evolve freely according to Hamiltonian (1) without any driven oscillations. We have acquired the output state ψ_{123} we want through this procedure.

By running computer simulation with oscillation amplitude $a = 0.05$, we discover that the transition times required are $\tau_{01} = 27.6\ ms$ and $\tau_{12} = 37.6\ ms$ respectively. The following figure is the evolution of the probability between the 3 states. The simulation was run in u_n space with $n = 20$. The choice of a large space was to ensure that all leakage of probability to higher excited states was calculated. Hence the error of the state construction scheme was properly accounted.

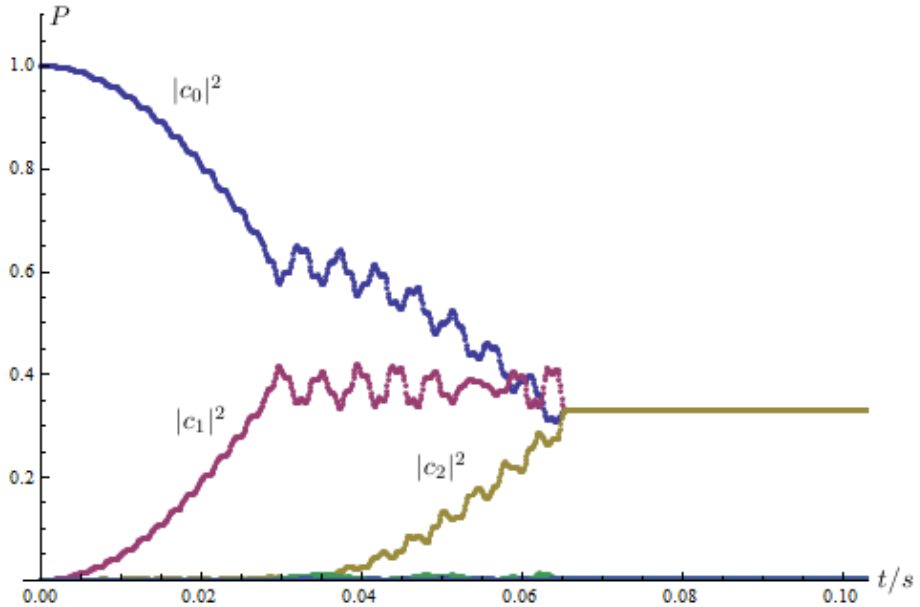

Figure 8: Probability evolution during state construction

Only $\sim 1\%$ of the probability leaks out of the 3 states. Therefore, the state construction result has $\sim 99\%$ accuracy. The deviations from our target 123-state are

$$|c_0|^2 - \frac{1}{3} = -0.0039 \qquad \frac{\delta|c_0|^2}{|c_0|^2} = -1.2\% \tag{45a}$$

$$|c_1|^2 - \frac{1}{3} = -0.0017 \qquad \frac{\delta|c_0|^2}{|c_0|^2} = -0.5\% \tag{45b}$$

$$|c_2|^2 - \frac{1}{3} = -0.0044 \qquad \frac{\delta|c_0|^2}{|c_0|^2} = -1.3\% \tag{45c}$$

$$1 - |c_0|^2 - |c_1|^2 - |c_2|^2 = 0.0101 \qquad \text{leakage} = 1.0\% \tag{45d}$$

Just for our interest, we would like to see the shape of the output state in real space:

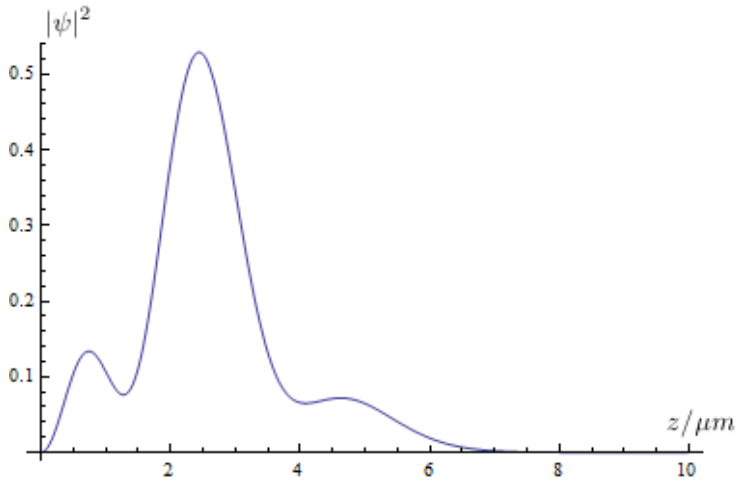

Figure 9: ψ_{123} in real space

5.2 Other Examples

Another state we are interested in is a state with 2 peaks at 2 distinct positions apart from each other. The probability of the neutron at either of the peak is approximately equal, with the probability at the center trough at $z \approx 0.41\ \mu m$ vanishes. Therefore we call this state a Schödinger's cat state, ψ_{cat}:

$$\psi_{cat}(t) = \frac{1}{\sqrt{4.2525}}\left(1.3u_0 + 0.75u_2 + u_3 + u_4\right) \tag{46}$$

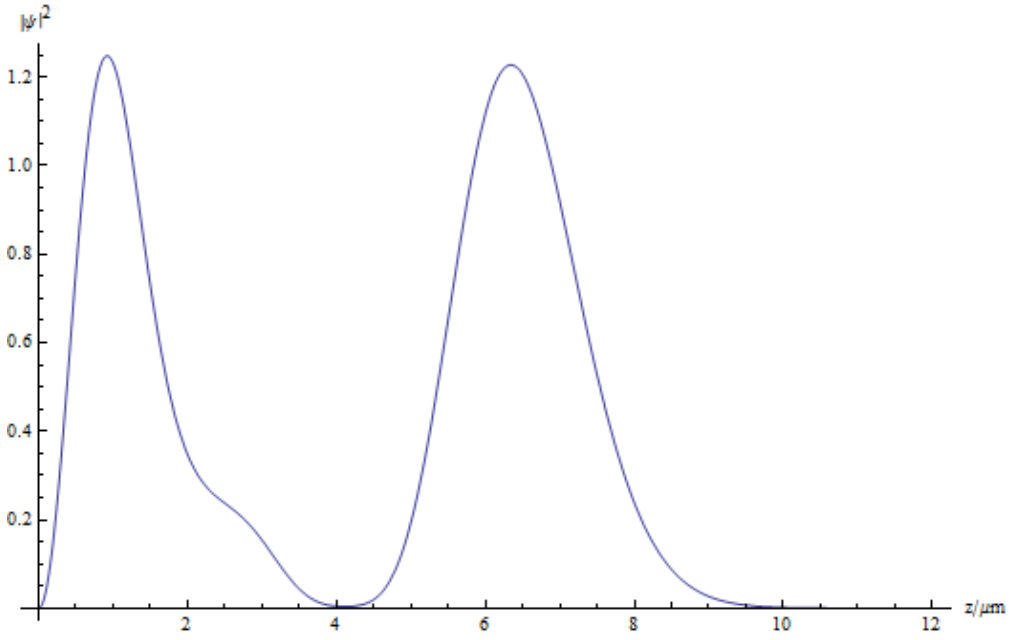

Figure 10: ψ_{cat} in real space at $t = 0$

Four states are utilized in this quantum superposition. Again starting from ground state u_0, we need to carry out four Rabi oscillations of frequencies $\Delta\omega_{40}$, $\Delta\omega_{30}$ and $\Delta\omega_{20}$ respectively. i.e. we use the following logistic to transport the probability amplitude from ground state the the nth excited states:

$$1.)\ u_0 \xrightarrow{\tau_{04}} u_4 \qquad 2.)\ u_0 \xrightarrow{\tau_{03}} u_3 \qquad 3.)\ u_0 \xrightarrow{\tau_{02}} u_2 \tag{47}$$

However, this time the constructed state involve high excited state u_4. The detuning of Rabi oscillation between u_4 and other more excited states are not large enough during u_0-u_4 oscillation. We need to lower the driving oscillation amplitude to prevent leakage of probability to other irrelevant states. We set $a = 0.005$, which is ten times smaller than our previous setting $a = 0.05$. This is at the expense of requiring $\sim$10 times more time t to construct our state.

Below is our result, the duration of the oscillation pulse are $\tau_{04} = 0.2210\ s$, $\tau_{03} = 0.2382\ s$, $\tau_{02} = 0.2259\ s$.

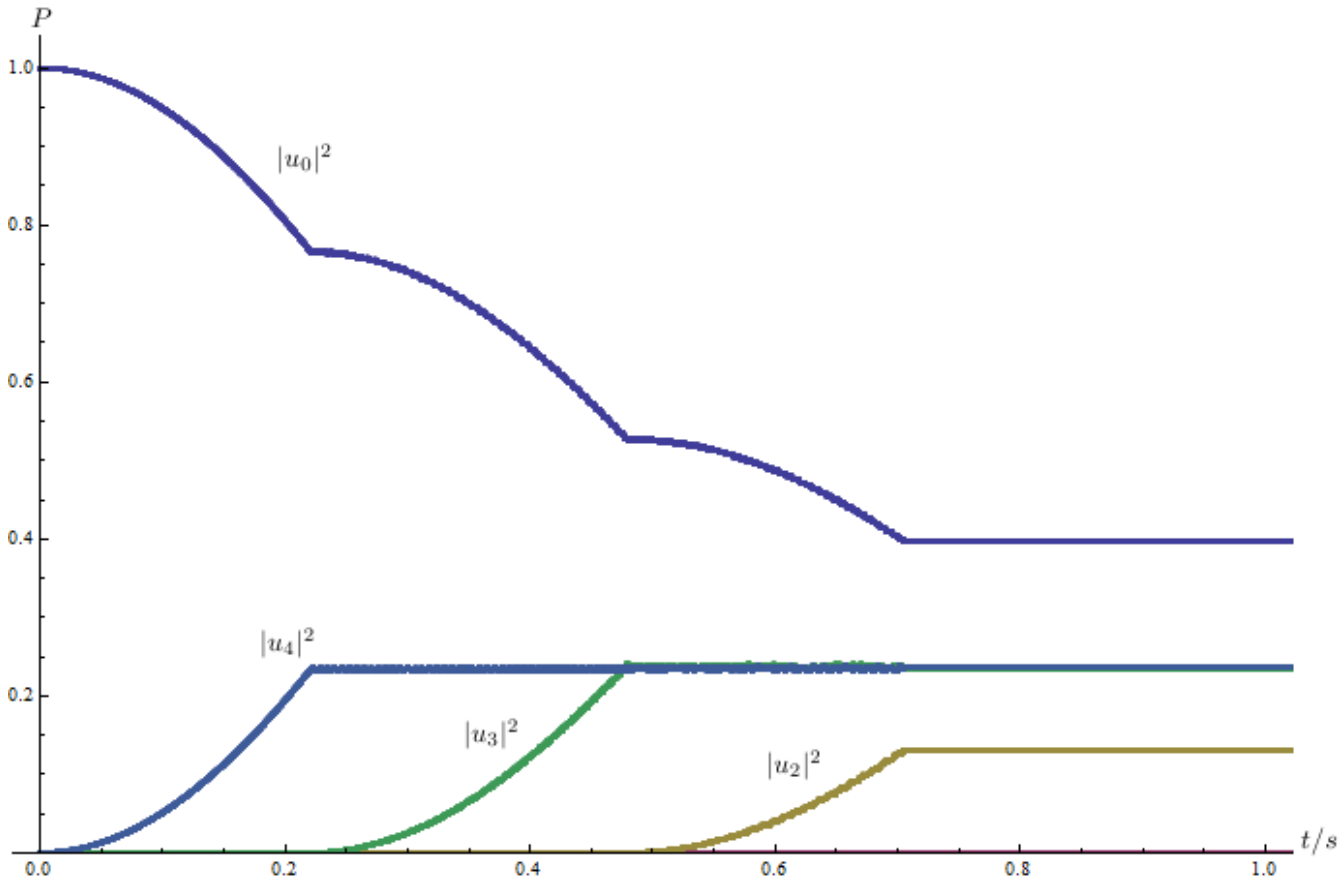

Figure 11: Construction of ψ_{cat} in u_n space

The average error of the probability amplitude of the states are $\sim 0.5\%$, calculated from the scheme in Eq. (45). The leakage of probability out of u_0, u_2, u_3 and u_4 is 0.14%. Hence, the error mostly comes from the oscillation between the four constituent states, but not from leakage to other irrelevant excited states.

Lastly, we want to see the shape of our output wavefunction ψ_{cat} in real space, which is at $t = 0.67\ s$. $\psi(t = 0.67\ s)$, in Fig. 12 , is nothing like the shape in Fig. 10. This is expected because ψ_{cat} is not an eigenstate of the Hamiltonian. The phase differences between each bases u_n will lead to a distortion of the wavefunction. Since we know that the wavefunction in Fig. 12 is definitely the wavefunction ψ_{cat} as we constructed it to be so, we expect the wavefunction to return to the shape of Fig. 10 after some characteristic period of time for ψ_{cat}. Indeed, the wavefunction return to its Schrödinger cat shape at $t = 0.74\ s$. And such pattern reoccurs for every $\sim 104\ s$, which is the characteristic period of this wavefunction.

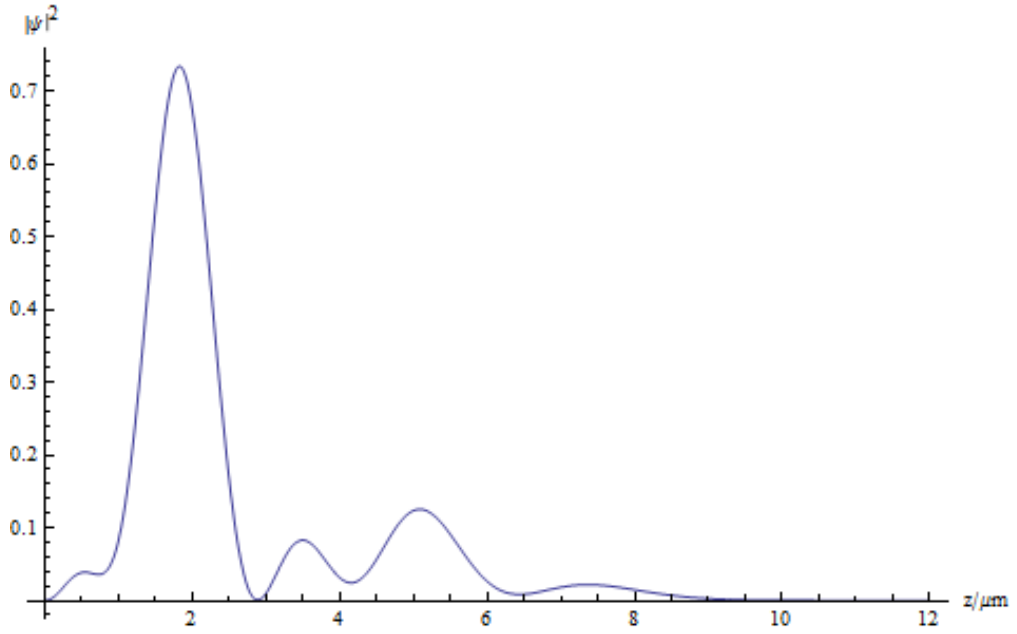

Figure 12: Real space probability shape of the output state at $t = 0.67\ s$

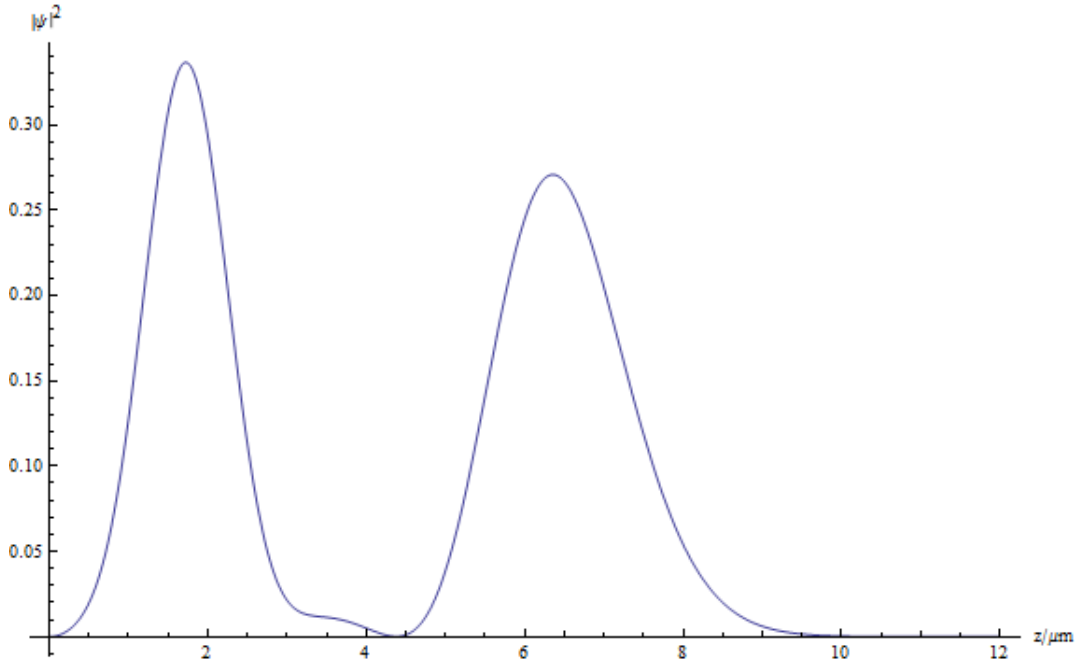

Figure 13: Real space probability shape of the output state at $t = 0.74\ s$

6 Conclusion

Upon the success of building the experiment setup of quantum bouncing ball system, a whole new area of neutron gravitational spectroscopy has been opened.

We have found that the behavior of quantum bouncing ball is analogue to a lot of quantum optics system. Quantum bouncing ball has its own set of bound states with discrete energy levels. While the energy level transition in atoms can be triggered by electromagnetic wave, transition between the energy levels in quantum bouncing ball system can be induced by an oscillation of the ground potential barrier.

Quantum bouncing can perform its own Rabi oscillation through driving the ground oscillation with certain resonance frequencies. Oscillation of the ground, corresponding to the oscillation of the neutron mirror in the experiment setup, can be manipulated without too much difficulty. Thus, it is not hard

to imagine one could construct specific wavefunction for the neutrons in quantum bouncing ball setup through controlling the neutron mirror's movement.

Indeed, we have shown that it is possible to construct particular wavefunction for quantum bouncing ball using the relation between ground oscillation and Rabi oscillation. We believe that one day such technique of state construction will be useful in the domain of quantum optics, gravitational spectroscopy, etc.

References

[1] H. Abele. "qBounce-realization of a quantum bouncing ball gravity spectrometer and new 5^{th} force limits". Mykonos, 2011.

[2] Katharina Durstberger-Rennhofer, Tobias Jenke, and Hartmut Abele. "Probing the neutron's electric neutrality with ramsey spectroscopy of gravitational quantum states of ultracold neutrons". Aug 2011.

[3] Julio Gea-Banacloche. "A quantum bouncing ball". Sept 1999.

[4] H. Leeb J. Schmiedmayer H. Abele, T. Jenke. "Ramsey's method of separated oscillating fields and its application to gravitationally induced quantum phase shifts". Mar 2010.

[5] *et al.* H. Abele. "Measurement of quantum states of neutrons in the earth's gravitational field". May 2003.